THE ASTROPHYSICAL JOURNAL, 178:347–369, 1972 December 1


# ROTATING BLACK HOLES: LOCALLY NONROTATING FRAMES, ENERGY EXTRACTION, AND SCALAR SYNCHROTRON RADIATION*

JAMES M. BARDEEN†
University of Washington, Seattle, Washington
AND
WILLIAM H. PRESS‡ AND SAUL A. TEUKOLSKY
California Institute of Technology, Pasadena, California
*Received 1972 June 5*

## ABSTRACT

This paper outlines and applies a technique for analyzing physical processes around rotating black holes. The technique is based on the orthonormal frames of "locally nonrotating observers." As one application of the technique, it is shown that the extraction of the rotational energy of a black hole, although possible in principle (e.g., the "Penrose-Christodoulou" process), is unlikely in any astrophysically plausible context. As another application, it is shown that, in order to emit "scalar synchrotron radiation," a particle must be highly relativistic as seen in the locally nonrotating frame—and can therefore not move along an astrophysically reasonable orbit. The paper includes a number of useful formulae for particle orbits in the Kerr metric, many of which have not been published previously.

## I. INTRODUCTION

Although there is as yet no certain observational identification of a black hole, the study of the properties of black holes and their interactions with surrounding matter is astrophysically important. Black-hole astrophysics is important for the following reasons. (i) At least some stars of mass $\gtrsim 2\ M_\odot$ probably fail to shed sufficient matter, when they die, to become white dwarfs or neutron stars, and instead collapse to form black holes. (ii) At least one irregularly pulsating X-ray source, Cygnus X-1, has been identified with a binary system which has a massive, invisible component; this might well be a black hole emitting X-rays as it accretes matter from its companion (for observations, see, e.g., Schreier *et al.* 1971 and Wade and Hjellming 1972). (iii) A black hole of $10^4$–$10^8\ M_\odot$ might lie at the center of the Galaxy and be responsible for radio and infrared phenomena observed there (Lynden-Bell and Rees 1971). (iv) Gravitational waves seem to have been detected coming from the direction of the galactic center with such intensity (Weber 1971 and references cited therein) that black-hole processes are the least unreasonable source. We are faced with a double mystery: first, puzzling observations; second, a poor theoretical understanding of what processes *might* occur near a black hole. Both sides of the mystery call for further theoretical work.

Most interactions of a black hole with its surroundings can be treated accurately by perturbation techniques, where the dynamics of matter, electromagnetic and gravitational waves takes place in the fixed background geometry generated by the

* Supported in part by the National Science Foundation [GP-15267] at the University of Washington, and [GP-28027, GP-27304] at the California Institute of Technology.

† Present address: Yale University, New Haven, Connecticut.

‡ Fannie and John Hertz Foundation Fellow.

hole. (Notable exceptions are the interactions of two or more black holes, or of black holes with neutron stars of comparable mass, and the highly nonspherical collapse of a star to form a black hole; currently there are no adequate techniques for treating such processes.) Most previous perturbation analyses have dealt with nonrotating (Schwarzschild) black holes. The static nature of the Schwarzschild metric and its spherical symmetry vastly simplify most problems. The orbits of particles can be described easily, and the theory of electromagnetic (Price 1972*a*) and gravitational (Zerilli 1971; Price 1972*b*) perturbations is well developed. A number of interesting model applications have begun to appear in the literature (Davis *et al.* 1971, 1972; Press 1971; Misner 1972*a*; Misner *et al.* 1972).

However, black holes in nature are likely to be highly rotating (Bardeen 1970*a*), and must therefore be described by the Kerr (1963) metric, rather than the Schwarzschild metric. Phenomena in the vicinity of a rotating black hole are considerably more complicated than in the nonrotating case. The metric is only stationary, not static, and only axisymmetric, not spherically symmetric. A complete description of particle orbits is rather complex (e.g., de Felice 1968; Carter 1968*a*). The equations governing electromagnetic and gravitational perturbations have only recently been separated into ordinary differential equations (Teukolsky 1972). The scalar wave equation has been known to be separable for some time, and has therefore been heavily relied on for qualitative perturbation results, even though there are no known classical scalar fields in nature.

A further difficulty is the complexity of coordinate systems for describing processes near a Kerr hole. Boyer-Lindquist (1967) coordinates are the natural generalization of Schwarzschild curvature coordinates and are the best for many purposes, but sufficiently close to the hole—in the "ergosphere"—they are somewhat unphysical. Example: Physical observers cannot remain "at rest" ($r$, $\theta$, $\varphi$ = constant).

In this paper we outline a method for treating physical processes in the Kerr geometry which has proved extremely fruitful in our research. The method, previously used by one of us for a different application (Bardeen 1970*b*), replaces coordinate frames by orthonormal tetrads (i.e., nonholonomic frames) which are carried by "locally nonrotating observers." In essence, the nonrotating observers are chosen to cancel out, as much as possible, the "frame-dragging" effects of the hole's rotation. They "rotate with the black hole" in such a way that physical processes as analyzed in their frame are far more transparent than in any coordinate frame. The method of locally nonrotating frames (LNRF), and the nature of the Kerr geometry as seen from the LNRF, are described in § III.

In § II, as a foundation for the LNRF description, we review properties of the Kerr metric and formulae for its particle orbits. While many of these results are known to those working in the field, many have not appeared in the literature; also we have used computer-assisted algebraic techniques, and other methods, to find equivalent formulae much simpler than many in the literature. These should prove useful to other investigators.

In § IV we apply the formalism of locally nonrotating frames to the question of synchrotron radiation (here, scalar synchrotron radiation) from particles in orbits near a black hole. (See Teukolsky 1972 for a proof that electromagnetic and gravitational synchrotron radiation are qualitatively the same as the scalar case.) This type of mechanism has been proposed by Misner (1972*a*) as a possible explanation for the intensity of Weber's observed radiation: a narrow synchrotron cone beamed in the galactic plane. We find that substantial beaming is possible only for particles in unstable, highly energetic orbits—orbits much more energetic than mere infall from infinity can produce. It is theoretically possible to extract energy from the rotating black hole itself (Penrose 1969; Christodoulou 1970). The LNRF methods give a clear picture of this energy extraction process, and make the process seem astro-

physically implausible. In particular, it seems unlikely that such extraction could realistically accelerate matter into a synchrotron-radiating orbit. These results make us pessimistic about the applicability of Misner's interesting synchrotron concept to any realistic astrophysical model.

In future papers, we will make use of methods described here to analyze more detailed and realistic processes near a rotating black hole.

## II. BASIC PROPERTIES OF THE KERR METRIC AND ITS ORBITS

We choose units with $G = c = 1$. In Boyer-Lindquist coordinates the metric is

$$ds^2 = -(1 - 2Mr/\Sigma)dt^2 - (4Mar \sin^2\theta/\Sigma)dtd\varphi + (\Sigma/\Delta)dr^2 + \Sigma d\theta^2 + (r^2 + a^2 + 2Ma^2r \sin^2\theta/\Sigma) \sin^2\theta d\varphi^2, \quad (2.1)$$

or, in contravariant form (matrix inverse),

$$\left(\frac{\partial}{\partial s}\right)^2 = -\frac{A}{\Sigma\Delta}\left(\frac{\partial}{\partial t}\right)^2 - \frac{4Mar}{\Sigma\Delta}\left(\frac{\partial}{\partial t}\right)\left(\frac{\partial}{\partial \varphi}\right) + \frac{\Delta}{\Sigma}\left(\frac{\partial}{\partial r}\right)^2 + \frac{1}{\Sigma}\left(\frac{\partial}{\partial \theta}\right)^2 + \frac{\Delta - a^2 \sin^2\theta}{\Sigma\Delta \sin^2\theta}\left(\frac{\partial}{\partial \varphi}\right)^2 . \quad (2.2)$$

Here $M$ is the mass of the black hole, $a$ is its angular momentum per unit mass ($0 \leq a \leq M$), and the functions $\Delta$, $\Sigma$, $A$ are defined by

$$\Delta \equiv r^2 - 2Mr + a^2 ,$$
$$\Sigma \equiv r^2 + a^2 \cos^2\theta ,$$
$$A \equiv (r^2 + a^2)^2 - a^2\Delta \sin^2\theta . \quad (2.3)$$

For $a = 0$, equations (2.1) and (2.2) reduce to the Schwarzschild solution in curvature coordinates.

It will be useful to express the metric (2.1) in the standard form valid for any stationary, axisymmetric, asymptotically flat spacetime—vacuum or nonvacuum—

$$ds^2 = -e^{2\nu}dt^2 + e^{2\psi}(d\varphi - \omega dt)^2 + e^{2\mu_1}dr^2 + e^{2\mu_2}d\theta^2 . \quad (2.4)$$

This standard metric becomes Kerr if

$$e^{2\nu} = \Sigma\Delta/A , \quad e^{2\psi} = \sin^2\theta A/\Sigma ,$$
$$e^{2\mu_1} = \Sigma/\Delta , \quad e^{2\mu_2} = \Sigma , \quad \omega = 2Mar/A . \quad (2.5)$$

The event horizon ("one-way membrane") is located at the outer root of the equation $\Delta = 0$,

$$r = r_+ \equiv M + (M^2 - a^2)^{1/2} \quad (2.6)$$

for all $\theta, \varphi$. Over the range $0 \leq a \leq M$, $r_+$ varies from $2M$ to $M$. The static limit (outer boundary of the ergosphere) is at the outer root of $(\Sigma - 2Mr) = 0$,

$$r = r_0 \equiv M + (M^2 - a^2 \cos^2\theta)^{1/2} . \quad (2.7)$$

A physical observer—i.e., one who follows a timelike world line—must be dragged in the positive $\varphi$ direction if he is inside the static limit. Observers inside the static limit, i.e., in the ergosphere, have access to the "negative energy trajectories" which extract energy from the black hole (see § III).

The general orbits of particles (or photons) in the Kerr geometry are described by three constants of motion (Carter 1968*a*). In terms of the covariant Boyer-Lindquist

components of the particle's 4-momentum at some instant, these conserved quantities are

$$E = -p_t = \text{total energy},$$

$$L = p_\varphi = \text{component of angular momentum parallel to symmetry axis},$$

$$Q = p_\theta^2 + \cos^2\theta[a^2(\mu^2 - p_t^2) + p_\varphi^2/\sin^2\theta]. \tag{2.8}$$

Here $\mu$ is the rest mass of the particle ($\mu = 0$ for photons), which is a trivial fourth constant of the motion. Note that $Q = 0$ is a necessary and sufficient condition for motion initially in the equatorial plane to remain in the equatorial plane for all time. Any orbit which crosses the equatorial plane has $Q > 0$. When $a = 0$, $Q + p_\varphi^2$ is the square of the total angular momentum. By solving equation (2.8) for the $p_\mu$'s and thence the $p^\mu$'s, one obtains equations governing the orbital trajectory,

$$\Sigma \frac{dr}{d\lambda} = \pm(V_r)^{1/2}, \tag{2.9a}$$

$$\Sigma \frac{d\theta}{d\lambda} = \pm(V_\theta)^{1/2}, \tag{2.9b}$$

$$\Sigma \frac{d\varphi}{d\lambda} = -(aE - L/\sin^2\theta) + aT/\Delta, \tag{2.9c}$$

$$\Sigma \frac{dt}{d\lambda} = -a(aE\sin^2\theta - L) + (r^2 + a^2)T/\Delta. \tag{2.9d}$$

Here $\lambda$ is related to the particle's proper time by $\lambda = \tau/\mu$, and is an affine parameter in the case $\mu \to 0$, and

$$\begin{aligned} T &\equiv E(r^2 + a^2) - La, \\ V_r &\equiv T^2 - \Delta[\mu^2 r^2 + (L - aE)^2 + Q], \\ V_\theta &\equiv Q - \cos^2\theta[a^2(\mu^2 - E^2) + L^2/\sin^2\theta]. \end{aligned} \tag{2.10}$$

Without loss of generality one is free to take $\mu = 1$ for particles and $\mu = 0$ for photons, in equations (2.8), (2.9), (2.10). (For particles this merely renormalizes $E$, $L$, and $Q$ to a "per unit rest mass" basis.) $V_r$ and $V_\theta$ are "effective potentials" governing particle motions in $r$ and $\theta$. Notice that $V_r$ is a function of $r$ only, $V_\theta$ is a function of $\theta$ only, and consequently equations (2.9a) and (2.9b) form a decoupled pair. Also, it is not difficult to show (Wilkins 1972) that if $E/\mu < 1$ the orbit is bound (does not reach $r = \infty$), while all orbits with $E/\mu > 1$ are unbound except for a "measure-zero" set of unstable orbits.

The single most important class of orbits are the circular orbits in the equatorial plane. For a circular orbit at some radius $r$, $dr/d\lambda$ must vanish both instantaneously and at all subsequent times (orbit at a perpetual turning point). Equation (2.9a) then gives the conditions

$$V_r(r) = 0, \qquad V_r'(r) = 0. \tag{2.11}$$

These equations can be solved simultaneously for $E$ and $L$ to give

$$E/\mu = \frac{r^{3/2} - 2Mr^{1/2} \pm aM^{1/2}}{r^{3/4}(r^{3/2} - 3Mr^{1/2} \pm 2aM^{1/2})^{1/2}}, \tag{2.12}$$

$$L/\mu = \frac{\pm M^{1/2}(r^2 \mp 2aM^{1/2}r^{1/2} + a^2)}{r^{3/4}(r^{3/2} - 3Mr^{1/2} \pm 2aM^{1/2})^{1/2}}. \tag{2.13}$$

In these and all subsequent formulae, the upper sign refers to direct orbits (i.e., corotating with $L > 0$), while the lower sign refers to retrograde orbits (counter-rotating with $L < 0$). For an extreme-rotating black hole, $a = M$, equations (2.12) and (2.13) simplify somewhat,

$$E/\mu = \frac{r \pm M^{1/2}r^{1/2} - M}{r^{3/4}(r^{1/2} \pm 2M^{1/2})^{1/2}}, \qquad \text{for } a = M; \tag{2.14}$$

$$L/\mu = \frac{\pm M(r^{3/2} \pm M^{1/2}r + Mr^{1/2} \mp M^{3/2})}{r^{3/4}(r^{1/2} \pm 2M^{1/2})^{1/2}}, \qquad \text{for } a = M. \tag{2.15}$$

The coordinate angular velocity of a circular orbit is

$$\Omega \equiv d\varphi/dt = \pm M^{1/2}/(r^{3/2} \pm aM^{1/2}). \tag{2.16}$$

Circular orbits do not exist for all values of $r$. The denominator of equations (2.12) and (2.13) is real only if

$$r^{3/2} - 3Mr^{1/2} \pm 2aM^{1/2} \geq 0. \tag{2.17}$$

The limiting case of equality gives an orbit with infinite energy per unit rest mass, i.e., a photon orbit. This photon orbit is the innermost boundary of the circular orbits for particles; it occurs at the root of (2.17),

$$r = r_{\rm ph} \equiv 2M\{1 + \cos[\tfrac{2}{3}\cos^{-1}(\mp a/M)]\}. \tag{2.18}$$

For $a = 0$, $r_{\rm ph} = 3M$, while for $a = M$, $r_{\rm ph} = M$ (direct) or $4M$ (retrograde).

For $r > r_{\rm ph}$ not all circular orbits are bound. An unbound circular orbit is one with $E/\mu > 1$. Given an infinitesimal outward perturbation, a particle in such an orbit will escape to infinity on an asymptotically hyperbolic trajectory. The unbound circular orbits are circular in geometry but hyperbolic in energetics, and they are all unstable. Bound circular orbits exist for $r > r_{\rm mb}$, where $r_{\rm mb}$ is the radius of the marginally bound ("parabolic") circular orbit with $E/\mu = 1$,

$$r_{\rm mb} = 2M \mp a + 2M^{1/2}(M \mp a)^{1/2}. \tag{2.19}$$

Note also that $r_{\rm mb}$ is the minimum perihelion of all parabolic ($E/\mu = 1$) orbits. In astrophysical problems, particle infall from infinity is very nearly parabolic, since the velocities of matter at infinity satisfy $v \ll c$. Any parabolic trajectory which penetrates to $r < r_{\rm mb}$ must plunge directly into the black hole. For $a = 0$, $r_{\rm mb} = 4M$; for $a = M$, $r_{\rm mb} = M$ (direct) or $5.83M$ (retrograde).

Even the bound circular orbits are not all stable. Stability requires that $V_r''(r) \leq 0$, which yields the three equivalent conditions

$$1 - (E/\mu)^2 \geq \tfrac{2}{3}(M/r),$$

$$r^2 - 6Mr \pm 8aM^{1/2}r^{1/2} - 3a^2 \geq 0,$$

or

$$r \geq r_{\rm ms}, \tag{2.20}$$

where $r_{\rm ms}$ is the radius of the marginally stable orbit,

$$r_{\rm ms} = M\{3 + Z_2 \mp [(3 - Z_1)(3 + Z_1 + 2Z_2)]^{1/2}\},$$
$$Z_1 \equiv 1 + (1 - a^2/M^2)^{1/3}[(1 + a/M)^{1/3} + (1 - a/M)^{1/3}],$$
$$Z_2 \equiv (3a^2/M^2 + Z_1^2)^{1/2}. \tag{2.21}$$

For $a = 0$, $r_{\rm ms} = 6M$; for $a = M$, $r_{\rm ms} = M$ (direct) or $9M$ (retrograde). Figure 1

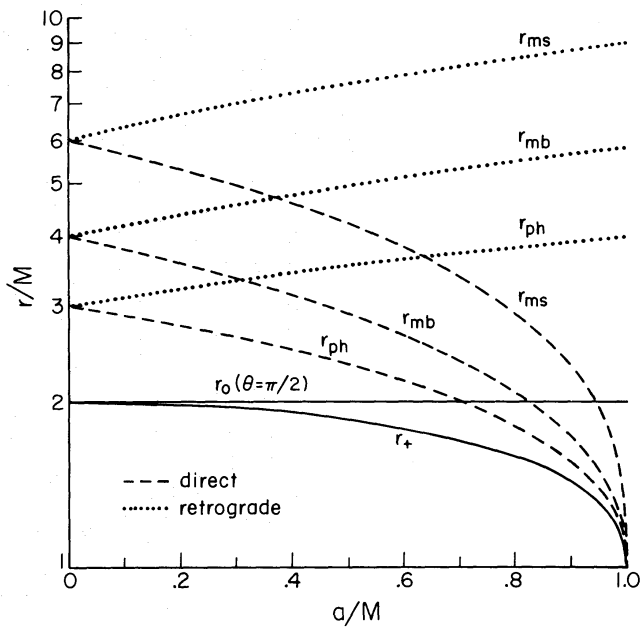


FIG. 1.—Radii of circular, equatorial orbits around a rotating black hole of mass $M$, as functions of the hole's specific angular momentum $a$. Dashed and dotted curves (for direct and retrograde orbits) plot the Boyer-Lindquist coordinate radius of the innermost stable (ms), innermost bound (mb), and photon (ph) orbits. Solid curves indicate the event horizon ($r_+$) and the equatorial boundary of the ergosphere ($r_0$).

shows the radii $r_+$, $r_0(\theta = \pi/2)$, $r_{ph}$, $r_{mb}$, and $r_{ms}$ as functions of $a$ for direct and retrograde orbits.

For $a = M$, $r_+ = r_{ph} = r_{mb} = r_{ms} = M$, and it appears that the photon, marginally bound, and marginally stable orbits are coincident with the horizon. Appearances are deceptive! The horizon is a null hypersurface, and no timelike curves can lie in it. The confusion is due to the subtle nature of the Boyer-Lindquist coordinates at $r = M$ for $a = M$. In fact the orbits at $r_{ph}$, $r_{mb}$, and $r_{ms}$ are all outside the horizon and all distinct. Figure 2 illustrates the nature of the problem; it shows schematically the equatorial plane embedded in a Euclidean 3-space, for $a/M = 0.9$, 0.99, 0.999, and 1. In the limit $a \to M$ the orbits at $r_{ph}$, $r_{mb}$, and $r_{ms}$ remain separated in proper radial distance, but the entire section of the manifold $r \leq r_{ms}$ becomes singularly projected into the Boyer-Lindquist coordinate location $r = M$. In the limit $a \to M$, the proper radial distance between $r_{ms}$ and $r_{mb}$ goes to infinity, as does that between $r_{ms}$ and $r_0$. The proper distance between $r_{mb}$ and $r_{ph}$ remains finite and nonzero, as does that between $r_{ph}$ and $r_+$. (The infinities are not physically important; an infalling particle follows a timelike curve, while the infinite distances are in a spacelike direction.)

For astrophysical applications with $a$ very close to $M$ (see Bardeen 1970*a*), one often needs to know explicitly the limiting behavior of $r_+$, $r_{ph}$, $r_{mb}$, and $r_{ms}$. Let $a = M(1 - \delta)$; then

$$r_+ \approx M[1 + (2\delta)^{1/2}], \qquad r_{ph} \approx M[1 + 2(\tfrac{2}{3}\delta)^{1/2}],$$
$$r_{mb} \approx M[1 + 2\delta^{1/2}], \qquad r_{ms} \approx M[1 + (4\delta)^{1/3}]. \tag{2.22}$$

Using these formulae, one finds that the proper radial distance between $r_+$ and $r_{ph}$ becomes $\frac{1}{2}M \ln 3$, that between $r_{ph}$ and $r_{mb}$ becomes $M \ln [(1 + 2^{1/2})/3^{1/2}]$, and that between $r_{mb}$ and $r_{ms}$ becomes $M \ln [2^{7/6}(2^{1/2} - 1)\delta^{-1/6}]$ in the limit $\delta \to 0$.

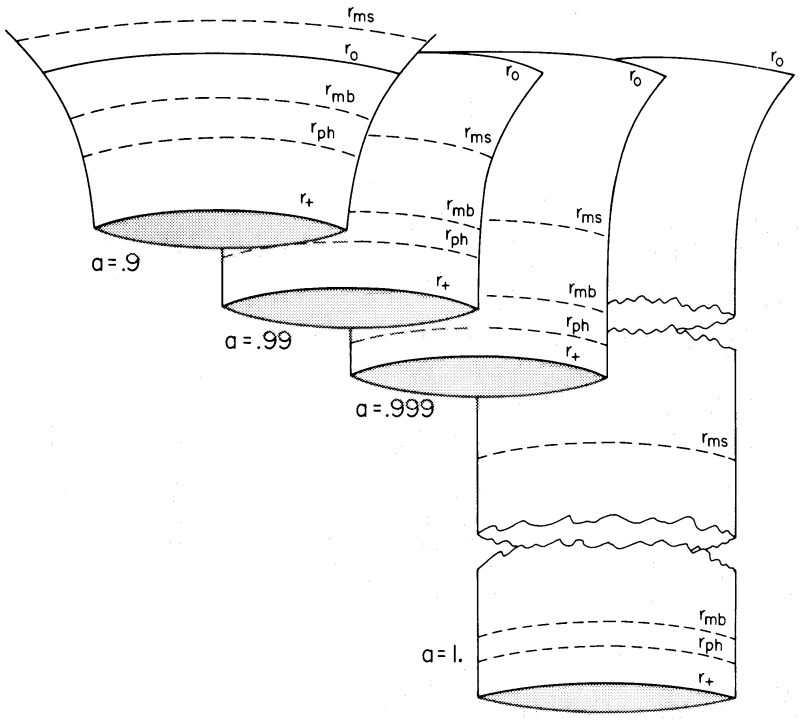


FIG. 2.—Embedding diagrams of the "plane" $\theta = \pi/2$, $t$ = constant, for rotating black holes with near-maximum angular momentum. Here $a$ denotes the hole's angular momentum in units of $M$. The Boyer-Lindquist radial coordinate $r$ determines only the circumference of the "tube." When $a \to M$, the orbits at $r_{ms}$, $r_{mb}$, and $r_{ph}$ all have the same circumference and coordinate radius, although—as the embedding diagram shows clearly—they are in fact distinct.

The orbits at $r = M$ are distinct energetically as well as geometrically. By taking appropriate limits of equations (2.12) and (2.13), one obtains

$$E/\mu \to 3^{-1/2}, \quad L/\mu \to 2M/3^{1/2} \quad \text{at } r = r_{ms} \text{ as } a \to M,$$
$$E/\mu \to 1, \quad L/\mu \to 2M \quad \text{at } r = r_{mb} \text{ as } a \to m,$$
$$E/\mu \to \infty, \quad L/\mu \to 2ME/\mu \quad \text{at } r = r_{ph} \text{ as } a \to M. \tag{2.23}$$

A clearer picture of the relations among these various orbits, and among general orbits in the equatorial plane, will emerge in our consideration of locally nonrotating frames.

## III. LOCALLY NONROTATING FRAMES

For any stationary, axisymmetric, asymptotically flat spacetime (for which the metric can always be written in the standard form of eq. [2.4]), it is useful to introduce a set of local observers who, in some sense, "rotate with the geometry" (Bardeen 1970*b*). Each observer carries an orthonormal tetrad of 4-vectors, his locally Minkowskian coordinate basis vectors. Rather than describe physical quantities (vectors, tensors, etc.) by their coordinate components at each point, one describes them by their projections on the orthonormal tetrad, i.e., their physically measured components in the local observer's frame. The desideratum governing the choice of observers is that physical processes described in their frames appear "simple." Physics is *not* simple in the Boyer-Lindquist coordinate frames because (i) the dragging of inertial frames becomes so severe that the $t$ coordinate basis vector $(\partial/\partial t)$ goes space-

like at the static limit $r_0$, and (ii) the metric is nondiagonal, so raising and lowering tensor indices typically introduces algebraic complexity.

For metrics in the standard form (2.4), there is a uniquely sensible choice of observers and tetrads: the locally nonrotating frames (LNRF) for which the observers' world lines are $r$ = constant, $\theta$ = constant, $\varphi = \omega t$ + constant. Here $\omega = -g_{\varphi t}/g_{\varphi\varphi}$ is the function appearing in equation (2.5). The orthonormal tetrad carried by such an observer (the set of LNRF basis vectors) at the point $t$, $r$, $\theta$, $\varphi$ is given by

$$\begin{aligned}
\boldsymbol{e}_{(t)} &= e^{-\nu}\left(\frac{\partial}{\partial t} + \omega\frac{\partial}{\partial\varphi}\right) = \left(\frac{A}{\Sigma\Delta}\right)^{1/2}\frac{\partial}{\partial t} + \frac{2Mar}{(A\Sigma\Delta)^{1/2}}\frac{\partial}{\partial\varphi}\,,\\
\boldsymbol{e}_{(r)} &= e^{-\mu_1}\frac{\partial}{\partial r} = \left(\frac{\Delta}{\Sigma}\right)^{1/2}\frac{\partial}{\partial r}\,,\\
\boldsymbol{e}_{(\theta)} &= e^{-\mu_2}\frac{\partial}{\partial\theta} = \frac{1}{\Sigma^{1/2}}\frac{\partial}{\partial\theta}\,,\\
\boldsymbol{e}_{(\varphi)} &= e^{-\psi}\frac{\partial}{\partial\varphi} = \left(\frac{\Sigma}{A}\right)^{1/2}\frac{1}{\sin\theta}\frac{\partial}{\partial\varphi}\,.
\end{aligned} \tag{3.1}$$

Here the first expression for each basic vector is valid for any spacetime with the standard metric (2.4); the second expression specializes to the Kerr metric. The corresponding basis of one-forms (or covariant basis vectors) is

$$\begin{aligned}
\boldsymbol{e}^{(t)} &= e^{\nu}\boldsymbol{dt} = (\Sigma\Delta/A)^{1/2}\boldsymbol{dt}\,,\\
\boldsymbol{e}^{(r)} &= e^{\mu_1}\boldsymbol{dr} = (\Sigma/\Delta)^{1/2}\boldsymbol{dr}\,,\\
\boldsymbol{e}^{(\theta)} &= e^{\mu_2}\boldsymbol{d\theta} = \Sigma^{1/2}\boldsymbol{d\theta}\,,\\
\boldsymbol{e}^{(\varphi)} &= -\omega e^{\psi}\boldsymbol{dt} + e^{\psi}\boldsymbol{d\varphi} = -\frac{2Mar\sin\theta}{(\Sigma A)^{1/2}}\boldsymbol{dt} + \left(\frac{A}{\Sigma}\right)^{1/2}\sin\theta\boldsymbol{d\varphi}\,.
\end{aligned} \tag{3.2}$$

From equations (3.1) and (3.2) one reads off directly the Boyer-Lindquist components $e^{\mu}{}_{(i)}$ and $e_{\mu}{}^{(i)}$ of the LNRF basis vectors, since

$$\boldsymbol{e}_{(i)} = e^{\mu}{}_{(i)}\frac{\partial}{\partial x^{\mu}} \qquad \text{and} \qquad \boldsymbol{e}^{(i)} = e_{\mu}{}^{(i)}\boldsymbol{dx}^{\mu}\,. \tag{3.3}$$

As matrices $\|e^{\mu}{}_{(i)}\|$ and $\|e_{\mu}{}^{(i)}\|$, these components transform one back and forth between the LNRF frame and the Boyer-Lindquist coordinate frame. For example, the standard transformation law for components of a tensor reads

$$J_{(a)(b)} = e^{\mu}{}_{(a)}e^{\nu}{}_{(b)}J_{\mu\nu}\,, \qquad J_{\mu\nu} = e_{\mu}{}^{(a)}e_{\nu}{}^{(b)}J_{(a)(b)}\,. \tag{3.4}$$

The rotation one-forms, which allow one to read off the connection coefficients $\Gamma_{(a)(b)(i)}$ by $\boldsymbol{\omega}_{(a)(b)} = \Gamma_{(a)(b)(i)}\boldsymbol{e}^{(i)}$, are given by

$$\begin{aligned}
\boldsymbol{\omega}_{(t)(r)} &= -\nu_{,r}\exp(-\mu_1)\boldsymbol{e}^{(t)} - \tfrac{1}{2}\omega_{,r}\exp(\psi-\nu-\mu_1)\boldsymbol{e}^{(\varphi)}\,,\\
\boldsymbol{\omega}_{(t)(\theta)} &= -\nu_{,\theta}\exp(-\mu_2)\boldsymbol{e}^{(t)} - \tfrac{1}{2}\omega_{,\theta}\exp(\psi-\nu-\mu_2)\boldsymbol{e}^{(\varphi)}\,,\\
\boldsymbol{\omega}_{(t)(\varphi)} &= -\tfrac{1}{2}\omega_{,r}\exp(\psi-\nu-\mu_1)\boldsymbol{e}^{(r)} - \tfrac{1}{2}\omega_{,\theta}\exp(\psi-\nu-\mu_2)\boldsymbol{e}^{(\theta)}\,,\\
\boldsymbol{\omega}_{(r)(\theta)} &= \mu_{1,\theta}\exp(-\mu_2)\boldsymbol{e}^{(r)} - \mu_{2,r}\exp(-\mu_1)\boldsymbol{e}^{(\theta)}\,,\\
\boldsymbol{\omega}_{(r)(\varphi)} &= -\psi_{,r}\exp(-\mu_1)\boldsymbol{e}^{(\varphi)} + \tfrac{1}{2}\omega_{,r}\exp(\psi-\nu-\mu_1)\boldsymbol{e}^{(t)}\,,\\
\boldsymbol{\omega}_{(\theta)(\varphi)} &= -\psi_{,\theta}\exp(-\mu_2)\boldsymbol{e}^{(\varphi)} + \tfrac{1}{2}\omega_{,\theta}\exp(\psi-\nu-\mu_2)\boldsymbol{e}^{(t)}\,.
\end{aligned} \tag{3.5}$$

Here a comma denotes partial differentiation. (Note that $\boldsymbol{\omega}_{(a)(b)} = -\boldsymbol{\omega}_{(b)(a)}$.)

One indication of the simplicity of the LNRF is the simplicity of the Kerr geometry's Riemann tensor when expressed in LNRF components. Define the four quantities

$$Q_1 \equiv Mr(r^2 - 3a^2\cos^2\theta)/\Sigma^3\,, \qquad Q_2 \equiv Ma\cos\theta(3r^2 - a^2\cos^2\theta)/\Sigma^3\,,$$
$$S \equiv 3a\sin\theta\Delta^{1/2}(r^2 + a^2)/A\,, \qquad z = \Delta a^2\sin^2\theta/(r^2 + a^2)^2\,. \tag{3.6}$$

(The quantities $\Delta$, $\Sigma$, $A$ are defined by eq. [2.3].) Then one obtains

$$\begin{aligned}
R_{(t)(\varphi)(t)(\varphi)} &= -R_{(r)(\theta)(r)(\theta)} = Q_1\,,\\
R_{(t)(\varphi)(r)(\theta)} &= -Q_2\,,\\
R_{(t)(r)(t)(r)} &= -R_{(\varphi)(\theta)(\varphi)(\theta)} = -Q_1\frac{2+z}{1-z}\,,\\
R_{(t)(r)(t)(\theta)} &= R_{(\varphi)(r)(\varphi)(\theta)} = SQ_2\,,\\
R_{(t)(r)(\varphi)(r)} &= -R_{(t)(\theta)(\varphi)(\theta)} = SQ_1\,,\\
R_{(t)(r)(\varphi)(\theta)} &= -Q_2\frac{2+z}{1-z}\,,\\
R_{(t)(\theta)(t)(\theta)} &= -R_{(\varphi)(r)(\varphi)(r)} = Q_1\frac{1+2z}{1-z}\,,\\
R_{(t)(\theta)(\varphi)(r)} &= -Q_2\frac{1+2z}{1-z}\,.
\end{aligned} \tag{3.7}$$

The other nonzero components follow directly from the symmetries of the Riemann tensor. Notice that $Q_2$ vanishes in the equatorial plane; also, that the dependence on $z$ is always quite weak since

$$0 \le z \le 0.043$$

for all $r$, $\theta$, $a$ of interest ($r_+ \le r < \infty$, $0 \le \theta \le \pi$, $0 \le a \le M$).

At any instant in time, the local frame of *any* physical observer differs from the LNRF at the observer's location by a Lorentz transformation. One need only know the velocity of an observer relative to the LNRF, and the transformation formulae of special relativity, to obtain the Riemann tensor (or, similarly, any other physical quantity) in an arbitrary frame.

To use the LNRF in the analysis of processes in Kerr orbits, we must investigate the nature of the Kerr orbits as seen from the LNRF, i.e., their distribution in velocity space. In general, the 4-velocity $\boldsymbol{u}$ has the LNRF components

$$u^{(a)} = u^\mu e_\mu{}^{(a)}\,, \tag{3.8}$$

where the $u^\mu$ come from equation (2.9), and the $e_\mu{}^{(a)}$ from equation (3.2). The 3-velocity relative to the LNRF has components

$$\mathscr{V}^{(j)} = \frac{u^\mu e_\mu{}^{(j)}}{u^\nu e_\nu{}^{(t)}}\,, \qquad j = r, \theta, \varphi\,. \tag{3.9}$$

In particular, note that

$$\mathscr{V}^{(\varphi)} = e^{\psi-\nu}(\Omega - \omega)\,, \tag{3.10}$$

where $\Omega = u^\varphi/u^t$ as before. In the special case of circular, equatorial orbits, $\mathscr{V}^{(\varphi)}$ is the only nonvanishing velocity component, and is given by

$$\mathscr{V}^{(\varphi)} = \frac{\pm M^{1/2}(r^2 \mp 2aM^{1/2}r^{1/2} + a^2)}{\Delta^{1/2}(r^{3/2} \pm aM^{1/2})}\,. \tag{3.11a}$$

In the case $a = M$, equation (3.11a) further reduces to

$$\mathscr{V}^{(\varphi)} = \frac{\pm M^{1/2}(r^{3/2} \pm M^{1/2}r + Mr^{1/2} \mp M^{3/2})}{(r^{1/2} \pm M^{1/2})(r^{3/2} \pm M^{3/2})} . \tag{3.11b}$$

Corresponding to $\mathscr{V}^{(\varphi)}$, the quantity $\gamma \equiv (1 - [\mathscr{V}^{(\varphi)}]^2)^{-1/2}$ is given by

$$\gamma = \frac{\Delta^{1/2}(r^{3/2} \pm aM^{1/2})}{r^{1/4}(r^{3/2} - 3Mr^{1/2} \pm 2aM^{1/2})^{1/2}(r^3 + a^2r + 2Ma^2)^{1/2}} ; \tag{3.12a}$$

or for $a = M$,

$$\gamma = \frac{(r^{3/2} \pm M^{3/2})(r^{1/2} \pm M^{1/2})}{r^{1/4}(r^{1/2} \pm 2M^{1/2})^{1/2}(r^3 + M^2r + 2M^3)^{1/2}} . \tag{3.12b}$$

For all $a$, $\mathscr{V}^{(\varphi)}$ increases (but not monotonically!) from zero at $r = \infty$ to 1 (the speed of light) at the circular photon orbit $r = r_{\rm ph}$. Another interesting point is that $\mathscr{V}^{(\varphi)}(r = r_{\rm ms})$, the velocity of the most tightly bound circular orbit, goes to $\frac{1}{2}$ (not 1!) in the limit $a \to M$. The point once again is that for $a = M$, the marginally stable orbit and the photon orbit are distinct. The marginally bound orbit, also distinct, has $\mathscr{V}^{(\varphi)}(r = r_{\rm mb}) \to 2^{-1/2}$ for $a \to M$. In fact, *all* stable, bound orbits around a rotating black hole—except "plunge" orbits irrevocably approaching the horizon—have $|\mathscr{V}|$ substantially bounded away from 1. Consequently, a Lorentz transformation from an LNRF to a stable, bound orbital frame never brings in factors greater than order unity.

We now consider noncircular orbits in the equatorial plane ($Q = 0$; $E, L$ arbitrary). For each possible orbit, and at every radius $r$, we ask an LNRF observer to measure the velocity of the orbit at the instant that it passes him. The velocity is represented by a point in the $(\mathscr{V}^{(r)}, \mathscr{V}^{(\varphi)})$-plane, somewhere inside the speed-of-light circle $[\mathscr{V}^{(r)}]^2 + [\mathscr{V}^{(\varphi)}]^2 = 1$. Thus, certain regions of the two-dimensional velocity space at radius $r$ correspond to bound, stable orbits; other regions to hyperbolic orbits which escape to infinity; other regions to "plunge" orbits which go down the hole. Figure 3 shows a typical sequence of velocity-space diagrams corresponding to $a = 0.95M$ ($a = M$ would be similar, but would collapse several different interesting radii to $r = M$). The following types of orbits are delineated in figure 3: bound stable orbits which exist for $r > r_{\rm mb} \approx 1.94M$ (direct) or 8.86 (retrograde), denoted (B); plunge orbits originating at infinity, i.e., with $E/\mu \geq 1$, denoted (P); escape orbits which are the time reverse of (P) orbits, denoted (E) [since nothing can come out of the hole, some physical process near the hole is necessary to inject a particle into an (E) trajectory]; hyperbolic orbits which originate at infinity, and are scattered back to infinity by the hole (H); captured plunge orbits, i.e., plunge orbits with $E/\mu < 1$, denoted (C). Points on the border between regions (H) and (P) of velocity space correspond to unstable orbits, and the intersection of such a border with the line $\mathscr{V}^{(r)} = 0$ marks an unstable, unbound circular orbit.

Figure 3 also indicates the region of "negative energy states" first exploited by Penrose (1969). In the LNRF, a particle's 4-momentum has the flat-space form

$$\boldsymbol{p} = \mu(\gamma, \gamma\boldsymbol{\mathscr{V}}) , \qquad \gamma = (1 - \boldsymbol{\mathscr{V}}\cdot\boldsymbol{\mathscr{V}})^{-1/2} \tag{3.13}$$

and its conserved total energy (dot product of 4-momentum with the time-coordinate Killing vector) is

$$\begin{aligned} E &= -\boldsymbol{p}\cdot(\partial/\partial t) = -p_t = -p^{(a)}e_{t(a)} \\ &= \mu\gamma(e^{\nu} + \omega e^{\psi}\mathscr{V}^{(\varphi)}) , \end{aligned} \tag{3.14}$$

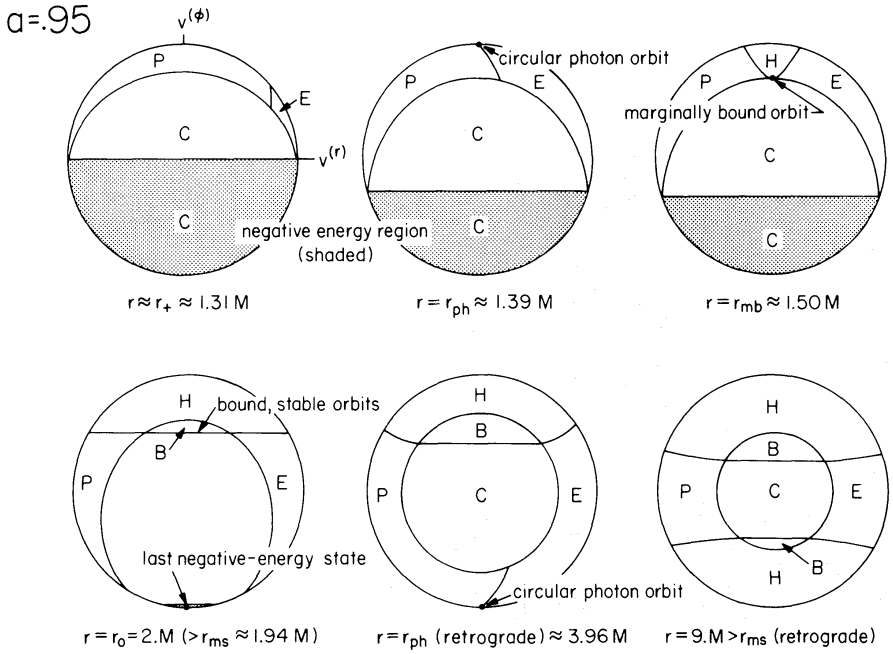


FIG. 3.—Distribution in velocity space of equatorial orbits passing through various radii $r$, around a rotating black hole with $a = 0.95M$. Each circle is the "space" of equatorial, ordinary velocities [$d$(proper distance)/$d$(proper time)] as measured in the proper reference frame of a locally nonrotating observer. The velocity circles are labeled by the radius $r$ of the observer. The center of each circle is zero velocity; the edge is the speed of light; the $\mathcal{V}^{(r)}$ direction corresponds to radial velocities, the $\mathcal{V}^{(\varphi)}$ direction to tangential velocities. A particle which passes the observer with its velocity in an E-region will escape to infinity. Similarly, P denotes plunge trajectories from infinity into the hole; C denotes "captured" plunges which could not have come from infinity; H denotes "hyperbolic" orbits from infinity and to infinity; B denotes bound, stable orbits which neither plunge nor escape. The shaded regions are the "negative energy" orbits (see text for details). Diagrams for other values of $a$ (the hole's specific angular momentum) are qualitatively similar.

so that in the equatorial plane,

$$E = \mu\gamma A^{-1/2}(r\Delta^{1/2} + 2Ma\mathcal{V}^{(\varphi)}) . \tag{3.15}$$

$E$ is negative for

$$\mathcal{V}^{(\varphi)} < -\frac{r(r^2 - 2Mr + a^2)^{1/2}}{2Ma} , \tag{3.16}$$

that is, below a horizontal line in the velocity plane. Outside the ergosphere this line fails to intersect the velocity-space circle, and there are no negative energy states. At the event horizon the line is $\mathcal{V}^{(\varphi)} = 0$. Negative energy trajectories are always captured plunges (C).

In the Penrose energy-extraction process, a body breaks up into two or more fragments; if any fragments are injected into negative energy orbits, the sum of the total energy of the remaining fragments is greater than the total energy of the original body, since $E$ is an additive conserved quantity. The extra energy comes from the rotational energy of the black hole (see Christodoulou 1970). Wheeler (1970) and others (see, e.g., Mashoon 1972) have speculated on the possibility that some natural astrophysical process, for example the breakup of a star by the tidal gravitational forces of the black hole, could result in the extraction of energy from the hole via the Penrose process. In the LNRF picture (fig. 3), the negative energy states and the (B)

orbits are always separated by a substantial velocity, even for $a \approx M$ and $r \approx M$. Thus, if a star is taken initially on a bound, stable orbit in the equatorial plane, there can be no energy extraction from its breakup unless hydrodynamical boosts of $\sim\frac{1}{2}$ the speed of light occur. Similar results hold if the initial orbit is taken to be a plunge orbit of any reasonable sort, i.e., one no more bound than the *most* bound (B) orbit.

Appendix A proves the general theorem which the LNRF picture makes plausible: If two trajectories differ in energy per unit rest mass by an amount of order unity, then their locally measured relative velocities differ by a substantial fraction of the speed of light. This result holds everywhere outside the event horizon (and even inside it, for that matter). The most bound plunge orbit that is astrophysically plausible has $E/\mu = 3^{-1/2}$ (minimum energy of a plunge orbit which results from the decay of a bound, stable orbit around any rotating black hole). Such an orbit is bounded away from the negative energy states by $|\mathscr{V}| \geq 0.5c$. Thus, energy extraction cannot be achieved unless hydrodynamical forces or superstrong radiation reactions can accelerate fragments to more than this speed during the infall. On dimensional grounds, such boosts seem to be excluded: Suppose a self-gravitating object of mass $m$ and radius $r$ falls into a black hole of mass $M$. The criterion for Roche breakup at radius $R$ is dimensionally

$$M/R^3 \sim m/r^3 . \tag{3.17}$$

After breakup, the object experiences tidal accelerations of magnitude $\sim r(M/R^3) \sim r(m/r^3)$ for a period of time $\sim(R^3/M)^{1/2} \sim (r^3/m)^{1/2}$, so the characteristic velocity of breakup is dimensionally

$$\mathscr{V} \sim (m/r)^{1/2} , \tag{3.18}$$

which is $\ll 1$ for any infalling object except highly bound neutron stars. Since equation (3.17) can be rewritten as

$$R/M = (r/m)(m/M)^{2/3} < 1 \qquad \text{if } m \ll M \text{ and } r \lesssim 10m , \tag{3.19}$$

for a neutron star falling into a substantially more massive black hole, the Roche limit is inside the event horizon. There will be no observable breakup at all.

As for the superstrong radiation reactions, we can only note that all calculations to date (e.g., Davis *et al.* 1971, 1972) show that energies radiated from plunge trajectories are typically

$$E_{\rm rad} \sim m(m/M) \ll m , \tag{3.20}$$

so that reaction boosts are of the order of

$$\mathscr{V} \sim (m/M)^{1/2} \ll 1 . \tag{3.21}$$

In the next section we consider the scalar wave equation in the Kerr background and find no evidence of any breakdown in the estimate (3.20) for astrophysically plausible processes.

## IV. THE SCALAR WAVE EQUATION AND SCALAR SYNCHROTRON RADIATION

The equation governing a scalar test field $\Phi$ in the Kerr background is

$$\Box\Phi = (-g)^{-1/2}[(-g)^{1/2}g^{\mu\nu}\Phi_{,\mu}]_{,\nu} = 4\pi T , \tag{4.1}$$

where $T$ is the density of scalar charge per proper volume as measured in the rest frame of the charge and $g = \det(g_{\mu\nu})$. A comma denotes partial (not covariant)

differentiation. In Boyer-Lindquist coordinates $(-g)^{1/2} = \Sigma \sin\theta$, and the metric $g^{\mu\nu}$ is given by equation (2.2); equation (4.1) becomes

$$\left\{\frac{\partial}{\partial r}\Delta\frac{\partial}{\partial r} + \frac{1}{\sin\theta}\frac{\partial}{\partial\theta}\sin\theta\frac{\partial}{\partial\theta} + \left(\frac{1}{\sin^2\theta} - \frac{a^2}{\Delta}\right)\frac{\partial^2}{\partial\varphi^2} - \frac{4Mar}{\Delta}\frac{\partial^2}{\partial\varphi\partial t} - \left[\frac{(r^2+a^2)^2}{\Delta} - a^2\sin^2\theta\right]\frac{\partial^2}{\partial t^2}\right\}\Phi = 4\pi\Sigma T\,. \quad (4.2)$$

Carter (1968*b*) first demonstrated the separability of equation (4.1), and the explicit separation of equation (4.2) has been given by Brill *et al.* (1972). The solutions have the form

$$\Phi = \sum_{lm}\int d\omega[R_{lm\omega}(r)S^m{}_l(-a^2\omega^2, \cos\theta)e^{im\varphi}e^{-i\omega t}]\,. \quad (4.3)$$

Here $S^m{}_l(-a^2\omega^2, \cos\theta)$ is the standard oblate spheroidal harmonic satisfying

$$\left(\frac{1}{\sin\theta}\frac{d}{d\theta}\sin\theta\frac{d}{d\theta} + \lambda_{ml} + a^2\omega^2\cos^2\theta - \frac{m^2}{\sin^2\theta}\right)S^m{}_l = 0\,, \quad (4.4)$$

where $\lambda_{ml}$ is the eigenvalue of $S^m{}_l$. We write $S^m{}_l(\theta)$ for $S^m{}_l(-a^2\omega^2, \cos\theta)$ and take the normalization

$$\int_{-1}^{+1} d(\cos\theta)\int_0^{2\pi} d\varphi|S^m{}_l(\theta)e^{im\varphi}|^2 = 1\,. \quad (4.5)$$

Substituting equations (4.3)–(4.5) into (4.2), one finds that the radial function $R_{lm\omega}$ satisfies

$$\left[\frac{d}{dr}\Delta\frac{d}{dr} + \frac{a^2m^2 - 4Marm\omega + (r^2+a^2)^2\omega^2}{\Delta} - \lambda_{ml} - a^2\omega^2\right]R_{lm\omega}(r) = \int_{-\infty}^{+\infty}\frac{d\omega}{2\pi}\int_{-1}^{1} d(\cos\theta)\int_0^{2\pi} d\varphi[e^{i\omega t}e^{-im\varphi}S^m{}_l(\theta)(4\pi\Sigma T)]\,. \quad (4.6)$$

Although $T$ is a scalar charge density, not a tensor gravitational source, one often seeks insight into gravitational-wave processes by taking $T$ to be the trace of the stress-energy tensor; i.e., one sets the fictitious scalar charge of a point particle equal in magnitude to its mass $\mu$. If the particle follows a world line $z^\mu(\tau)$, one has

$$T = \frac{\mu}{u^t}(-g)^{-1/2}\delta^3[x^i - z^i(\tau)] \qquad \text{for } i = r, \theta, \varphi\,, \quad (4.7)$$

where $u^t = dt/d\tau$. For a particle in an equatorial, circular orbit of radius $r_p$, with angular velocity $d\varphi/dt = \Omega$, this becomes

$$4\pi\Sigma T = \sum_{lm}(4\pi\mu/u^t)\delta(r - r_p)S^m{}_l(\theta)S^m{}_l(0)e^{-im\Omega t}e^{im\varphi}\,. \quad (4.8)$$

Thus, the Fourier-transformed source (right-hand side of eq. [4.6]) has nonvanishing $\omega$-components only for $\omega = m\Omega$, $m = 0, \pm1, \pm2, \ldots$. Further, if by convention we take the real part of $\Phi$ to be the physical field, then we can restrict attention to $\omega \geq 0$ without loss of generality, so that only positive $m$'s contribute if $\Omega > 0$, and negative if $\Omega < 0$. With this convention, the sum in equation (4.8) ranges from $m = 0$ to $m = \text{sgn}\,(\Omega)\infty$, and a factor 2 must be inserted on the right-hand side of (4.8) for $m \neq 0$.

Equation (4.6) can be simplified to an effective-potential equation by the introduction of a new coordinate $r^*$ such that

$$dr^*/dr = r^2/\Delta\,. \tag{4.9}$$

Explicitly,

$$r^* = r + M\ln\Delta + \frac{(2M^2 - a^2)}{2(M^2 - a^2)^{1/2}}\ln\left(\frac{r - r_+}{r - r_-}\right); \tag{4.10a}$$

or for $a = M$,

$$r^* = r + 2M\ln(r - M) - M^2/(r - M)\,. \tag{4.10b}$$

[Recall that $r_\pm = M \pm (M^2 - a^2)^{1/2}$.] If we put

$$\psi = rR_{lm\omega}\,, \tag{4.11a}$$

then equations (4.6) and (4.8) become

$$\frac{d^2\psi}{dr^{*2}} + W(r)\psi = \frac{8\pi\mu}{r_p u^t}S^m{}_l(0)\delta(r^* - r_p^*)\,, \tag{4.11b}$$

where $S^m{}_l(0) = S^m{}_l(-a^2m^2\Omega^2, 0)$ and $W(r)$ is the effective potential

$$W(r) = m^2\left[\frac{(r^2 + a^2)\Omega - a}{r^2}\right]^2 - \frac{\Delta}{r^4}\left[\lambda_{ml} - 2a\Omega m^2 + a^2\Omega^2m^2 + \frac{2(Mr - a^2)}{r^2}\right]. \tag{4.12}$$

Our boundary conditions for equation (4.11) agree with those of Misner (1972*b*), and we will not discuss them here, except for a brief summary in Appendix B. Misner and others use a slightly different $r^*$ coordinate, $r^*_n$ defined by

$$dr^*_n/dr = (r^2 + a^2)/\Delta$$

instead of equation (4.9). This $r^*_n$ has the conceptual advantage that $t \pm r^*_n$ are null coordinates, but the practical disadvantage that it makes equation (4.12) and subsequent equations somewhat more complicated.

Locally nonrotating frames give insight into the physical content of the separated wave equation (4.11). We eliminate $\Omega$ in favor of $\mathscr{V}$, the LNRF linear velocity of the orbiting particle as measured in a LNRF (in previous sections $\mathscr{V}$ was denoted $\mathscr{V}^{(\varphi)}$). It is useful to define a function $\mathscr{V}(r)$, the linear velocity of the frame rigidly rotating with angular velocity $\Omega$,

$$\mathscr{V}(r) = \frac{1}{r\Delta^{1/2}}[(r^3 + a^2r + 2Ma^2)\Omega - 2Ma]\,. \tag{4.13}$$

Thus, the particle's velocity is $\mathscr{V} = \mathscr{V}(r_p)$. Then equation (4.12) takes the simple form

$$W(r) = \frac{-\Delta}{r^4}\left[\lambda_{ml} - m^2\left(1 - \frac{1 - \mathscr{V}(r)^2}{1 + a^2/r^2 + 2Ma^2/r^3}\right) + \frac{2(Mr - a^2)}{r^2}\right]. \tag{4.14}$$

It is shown in Appendix C that $\lambda_{ml} \geq m^2$ for all physical cases. Since $\mathscr{V}(r_p) < 1$ and $Mr > a^2$ outside the horizon, $W(r_p) = O(m^2) < 0$. Thus, in the WKB limit of large barrier (large $m$), the field dies out exponentially as one moves radially away from the particle. Since $\mathscr{V}(r) \approx r\Omega \to \infty$ for large $r$, $W(r)$ becomes positive at some point $r_1 > r_p$, and traveling waves propagate from there to infinity. Similarly, $W(r)$ becomes positive at some point $r_2$, $r_+ < r_2 < r_p$, so traveling waves exist for $r < r_2$.

We are now in a position to discuss the interesting question of "beamed radiation" which was first raised by Misner (1972*a*). Two prerequisites for beamed radiation (i.e., radiation emitted into a solid angle much smaller than $4\pi$) are (i) that the source itself contain high multipoles ($l, m \gg 1$) and (ii) that the field coupled to these multipoles radiate to infinity in a relatively unimpeded manner. For a point source, condition (i) is satisfied, so (ii) becomes the essential condition to check. The WKB barrier factor which separates the source from its wave zone is

$$\exp\left[-\int_{r_2}^{r_1}[-W(r)]^{1/2}dr^*\right] \equiv \exp(-B)\,. \tag{4.15}$$

The question is: with $l \gg 1$, can $B$ be made small? We will see below that the *most* favorable case (the case of smallest $B$) is $m = l$. Appendix C derives the result

$$l^2 \leq \lambda_{ll} \leq l(l+1)\,; \tag{4.16}$$

so the effective potential (4.14) for $m = l$ is, with fractional errors of $O(1/l)$,

$$W(r) \simeq -\frac{l^2}{r^4}\Delta\frac{1-\mathscr{V}(r)^2}{1+a^2/r^2+2Ma^2/r^3} \qquad \text{for } l = m \gg 1\,. \tag{4.17}$$

The corresponding barrier-penetration factor for $m = l$ is

$$B \simeq l\int_{r_2}^{r_1}\frac{(1-\mathscr{V}(r)^2)^{1/2}}{(1+a^2/r^2+2Ma^2/r^3)^{1/2}(r^2-2Mr+a^2)^{1/2}}\,dr\,. \tag{4.18}$$

This barrier factor can be cast in a simple form by noticing that in the Kerr geometry, the proper circumferential radius $R_c$ and proper radial distance $R_p$ are given by

$$R_c = e^{\psi} = (r^2+a^2+2Ma^2/r)^{1/2}\,, \qquad dR_p/dr = (r^2/\Delta)^{1/2}\,. \tag{4.19}$$

So

$$B \simeq l\int_{r=r_2}^{r=r_1} R_c{}^{-1}(1-\mathscr{V}(r)^2)^{1/2}dR_p\,. \tag{4.20}$$

Large values of $l$ will contribute to the radiation field only if the integral in (4.20) is $\ll 1$. This requires two conditions: First,

$$1-\mathscr{V}(r_p)^2 \ll 1\,; \tag{4.21}$$

i.e., the particle orbit must be highly relativistic *as seen in the LNRF*. Second, $|\mathscr{V}(r)|$ must increase monotonically as $r$ increases from $r_p$ to $r_1$. [If it decreases initially, then $B$ cannot be made arbitrarily small even as $\mathscr{V}(r_p) \to 1$.] The fact that in the Kerr geometry, by contrast to flat space, the function $|\mathscr{V}(r)|$ can decrease with increasing $r$ is closely related to the existence of circular photon orbits. At radius $r$ the direction cosine relative to the $\varphi$-direction in the LNRF for a photon trajectory with energy $E$ and axial angular momentum $L$ is

$$\frac{p^{(\varphi)}}{p^{(t)}} = \frac{1}{(E/L-\omega)e^{\psi-\nu}} = \frac{1}{\mathscr{V}(r)}\,. \tag{4.22}$$

The quantity $\mathscr{V}(r)$ here is identical with that of equation (4.13) if $\Omega = E/L$. Since $|\mathscr{V}(r)|$ increases outward at $r = r_1$, with $|\mathscr{V}(r_1)| = 1$, the photon trajectory that is tangential there is at an inner turning point. Conversely, since $|\mathscr{V}(r)|$ decreases outward at $r = r_2$, the tangential photon trajectory is at an outer turning point. The photon orbit is circular at $r = r_1 = r_2$, if $|\mathscr{V}(r)|$ is independent of $r$ to first order near $r = r_1$. Thus if $r_p$ is inside the circular photon orbit, high multipoles will not

radiate to infinity even for $|\mathscr{V}| \to 1$. (In physical terms this is because, inside $r_{\rm ph}$, the radiation is beamed "down the hole.")

There are no nonplunge geodesic orbits inside $r_{\rm ph}$ in any case; but our results are equally valid for accelerated circular trajectories inside $r_{\rm ph}$, and for radiation emitted at pericenter by noncircular orbits and by accelerated trajectories in general. We can prove that no bound orbit satisfies $|\mathscr{V}| \to 1$ outside of $r_{\rm ph}$ as follows:

$$1 \geq E/\mu = -e^{t}{}_{(a)}u^{(a)} = (1 - \mathscr{V}^2)^{-1/2}(e^{\nu} + \omega e^{\psi}\mathscr{V}^{(\varphi)}) . \tag{4.23}$$

Since the last term in parentheses has no root outside $r_{\rm ph}$, $\mathscr{V}$ is bounded away from 1. Our conclusion is that high multipole radiation is suppressed exponentially with increasing $l$ for all astrophysically relevant equatorial orbits. There is no reason to believe that nonequatorial or noncircular orbits would be any more favorable than our arbitrarily accelerated circular trajectories.

Of course, there can be some *finite* beaming in the radiation by multipoles below the exponential cutoff. The characteristic $l$ of the cutoff is that $l$ for which $B \approx 1$. The most interesting cases are $r_p = r_{\rm ms}$ and $r_p = r_{\rm mb}$ in the limit $a \to M$, $l = m \gg 1$. In these cases equation (4.20) can be evaluated in terms of elementary functions with the results

$$B \approx 0.120l , \qquad r \to r_{\rm ms} , \tag{4.24a}$$

or $l_{\rm cutoff} \simeq 8$; and

$$B \approx 0.078l , \qquad r \to r_{\rm mb} , \tag{4.24b}$$

or $l_{\rm cutoff} \simeq 12$. In other cases, equation (4.20) (or [4.14] if $m < l$) can be integrated numerically. Figure 4 shows representative results with $a = M$ for various ratios $m/l$, for various geodesic circular orbits and circular accelerated trajectories chosen to be tangent to marginally bound ("parabolic") orbits at pericenter. One sees that $l = m$ is the case most favorable to propagation, and that the analytic results (4.24) correspond to the most favorable orbits. We have obtained similar results for various values of $a$, $0 \leq a \leq M$; the case $a = M$ is the most favorable to high multipoles.

Momentarily setting aside the question of astrophysical plausibility, it is interesting to see just how $l_{\rm cutoff} \to \infty$ as $\mathscr{V} \to 1$. Choose the origin for proper radial distance to be $R_p = 0$ at $r = r_p$, and expand $\mathscr{V}(r)$ in a Taylor series

$$\mathscr{V}(r) = \mathscr{V}\left[1 + \alpha\frac{R_p}{R_c} + \tfrac{1}{2}\beta\left(\frac{R_p}{R_c}\right)^2 + O\left(\frac{R_p}{R_c}\right)^3\right] . \tag{4.25}$$

Thus

$$[1 - \mathscr{V}(r)^2]^{1/2} \approx (1 - \mathscr{V}^2)^{1/2}\left(1 - 2\alpha\gamma^2\frac{R_p}{R_c} - \beta\gamma^2\frac{R_p{}^2}{R_c{}^2}\right)^{1/2} \tag{4.26}$$

when $\gamma = (1 - \mathscr{V}^2)^{-1/2} \gg 1$. The first-order term in equation (4.26) is sufficient to represent $(1 - \mathscr{V}^2)^{1/2}$ accurately over the whole range of integration of equation (4.20) if $\alpha\gamma \gg 1$. For most accelerated (nongeodesic) trajectories $\alpha$ is nonzero in the limit $\gamma \to \infty$ and one obtains

$$B \simeq \frac{l}{2\alpha\gamma^3}\int_0^1 (1 - x)^{1/2}dx = \frac{l}{3\alpha\gamma^3} , \tag{4.27}$$

or $l_{\rm cutoff} \simeq 3\alpha\gamma^3$. For geodesic orbits with $\gamma \gg 1$ (orbits just outside the circular photon orbit), $\alpha\gamma \ll 1$ and the second-order term is large relative to the first-order term over almost all of the range of integration. Therefore, in the latter case,

$$B \simeq \frac{l}{\beta^{1/2}\gamma^2}\int_0^1 (1 - x^2)^{1/2}dx = \frac{\pi}{4}\frac{l}{\beta^{1/2}\gamma^2} \tag{4.28}$$

and $l_{\rm cutoff} \simeq 4\pi^{-1}\beta^{1/2}\gamma^2$. In other words, there is a qualitative difference between

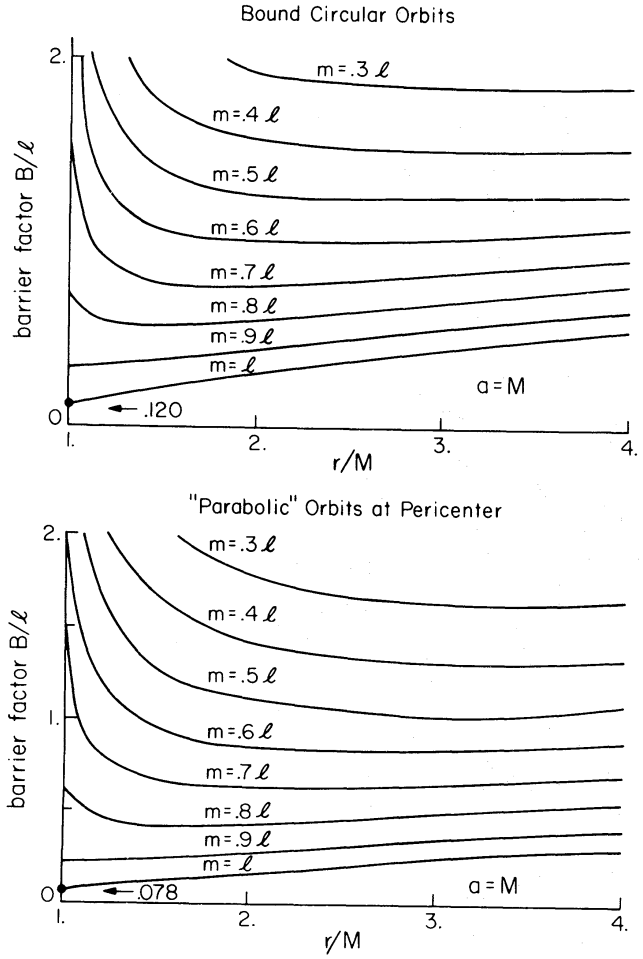


FIG. 4.—The "barrier factor" $B$ for (scalar) synchrotron-type radiation from stable orbits around an extreme-rotating black hole. In the WKB approximation (valid for high multipoles, $l \gg 1$), the power radiated in a given $l, m$ multipole is proportional to the exponential cutoff $\exp(-2B)$. Since $B/l$ is seen to be bounded away from zero, modes of high $l$ are always suppressed. The upper graph applies to stable, circular, geodesic orbits. The lower graph is computed for accelerated circular trajectories which are tangent to (and have the velocity of) marginally bound "parabolic" orbits at pericenter. We exclude extreme unbound orbits on the grounds of astrophysical implausibility (see text for details).

geodesic orbits and accelerated trajectories with the same LNRF velocity: the accelerated trajectories are more efficient sources of high-multipole radiation. In the Schwarzschild metric $\beta = 1$ at the circular photon orbit, while in the extreme ($a \simeq M$) Kerr metric $\beta = 12$ at the direct circular photon orbit ($r_p \simeq r_{\rm ph} \simeq M[1 + 2(\frac{2}{3}\delta)^{1/2}]$) and $\beta = \frac{75}{64}$ at the retrograde circular photon orbit ($r_p \simeq r_{\rm ph} = 4M$).

The locally nonrotating frame can also be used to interpret the radiation in the wave zone, $r > r_1$. As measured by an observer at rest in the LNRF at radius $r$ the scalar field oscillates with a proper frequency

$$\tilde{\Omega} = (\Omega - \omega)e^{-\nu} . \tag{4.29}$$

A photon with energy $E$ and axial angular momentum $L$ has a locally measured energy (frequency) in the LNRF

$$p^{(t)} = e^{-\nu}(E - \omega L) . \tag{4.30}$$

In particular, the frequency of a photon emitted tangent to the velocity-of-light circle at $r = r_1$, for which $E/L = \Omega$, changes in the same way with radius as the frequency of the scalar synchrotron radiation.

## V. CONCLUSION

Physical processes near a rotating black hole often reveal their underlying nature most clearly when they are examined in the locally nonrotating frames. In the case of rotational energy extraction, the LNRF picture points out the severe hydrodynamical constraints: energy extraction requires boosts of $\sim 0.5c$ in "short" hydrodynamical times. In the case of synchrotron radiation, the LNRF picture indicates that such beamed radiation is possible only from astrophysically implausible (unbound, unstable) orbits. The simplicity of the Riemann tensor in the LNRF picture points toward a number of future hydrodynamical applications. The physics of rotating black holes is sufficiently rich and varied as to require a variety of techniques, among which the LNRF picture is, we think, an important one.

We thank Paul Chrzanowski, Charles W. Misner, and Larry Smarr for valuable discussions and for making unpublished work available to us. We thank Kip S. Thorne for advice on preparing the manuscript.

## APPENDIX A

## BOUNDS ON ENERGIES AND RELATIVE VELOCITIES OF PARTICLE ORBITS

Consider a particle of rest mass $\mu$ and conserved energy $E = -\boldsymbol{p}\cdot\boldsymbol{\xi}_t$, where $\boldsymbol{p}$ is the 4-momentum and $\boldsymbol{\xi}_t$ is the time Killing vector. Not all values of $E/\mu$ are possible for trajectories through a given point in spacetime. For example, particles at radial infinity must have $E/\mu \geq 1$. We first ask, what is the bound on $E/\mu$ for a general point?

Pick an orthonormal frame at the point. The 4-velocity of a particle has components $\boldsymbol{u} = (\gamma, \gamma\boldsymbol{v})$ with $\boldsymbol{v}$ a 3-vector and $\gamma = (1 - \boldsymbol{v}^2)^{-1/2}$; the time Killing vector has components $\boldsymbol{\xi}_t = (\xi_0, \boldsymbol{\xi})$, with $\boldsymbol{\xi}$ a 3-vector. The particle's ratio of energy to rest mass is given by

$$E/\mu = -\boldsymbol{u}\cdot\boldsymbol{\xi}_t = \gamma(\xi_0 - \boldsymbol{v}\cdot\boldsymbol{\xi}) , \tag{A1}$$

where the dot denotes the scalar product in the local Euclidean 3-space. Evidently, a necessary (but not a sufficient) condition for an extremum (hence a bound) on $E/\mu$ is

$$\boldsymbol{v}\cdot\boldsymbol{\xi} = \pm v\xi , \tag{A2}$$

where $v = |\boldsymbol{v}|$, $\xi = |\boldsymbol{\xi}|$. Now we distinguish two cases: If $\boldsymbol{\xi}_t$ is spacelike (e.g., in the ergosphere of the Kerr geometry), then we have $\xi_0 < \xi$; and inspection of equation (A1) shows that all values of $E/\mu$ are possible,

$$-\infty < E/\mu < +\infty \qquad \text{for } \boldsymbol{\xi}_t \text{ spacelike} . \tag{A3}$$

The infinite limits correspond to $v \to 1$ with the two signs of equation (A2). If, instead, $\boldsymbol{\xi}_t$ is timelike (e.g., at radial infinity), so that $\xi_0 > \xi$, then the right-hand side of equation (A1) is always positive, and there is a nontrivial lower bound on $E/\mu$. Rewriting equation (A1) and using equation (A2) with the upper sign, we obtain

$$(\xi^2 + E^2/\mu^2)v^2 - 2\xi\xi_0 v + (\xi_0{}^2 - E^2/\mu^2) = 0 . \tag{A4}$$

The extremum in $E/\mu$ is obtained by setting the discriminant of this equation, a quadratic in $v$, equal to zero; this gives

$$0 = (E/\mu)^2[(E/\mu)^2 - \xi^2 + {\xi_0}^2] . \tag{A5}$$

The root $E/\mu = 0$ is spurious, and the lower bound on $E/\mu$ is

$$(E/\mu)^2 = {\xi_0}^2 - \xi^2 = -\boldsymbol{\xi}_t \cdot \boldsymbol{\xi}_t . \tag{A6}$$

We see that the allowed range of $E/\mu$ at a point depends only on the norm of the time Killing vector at that point,

$$(-\boldsymbol{\xi}_t \cdot \boldsymbol{\xi}_t)^{1/2} \leq E/\mu < +\infty \qquad \text{for } \boldsymbol{\xi}_t \text{ timelike} . \tag{A7}$$

Finally note that the two cases (A3) and (A7) imply as a general condition,

$$(E/\mu)^2 + \boldsymbol{\xi}_t \cdot \boldsymbol{\xi}_t > 0 . \tag{A8}$$

Now turn to a different problem: If two orbits through a point have different ratios of energy to rest mass, $E_1/\mu_1$ and $E_2/\mu_2$, they have different 4-velocities and therefore a nonzero relative 3-velocity, $|w|$ (velocity of one particle seen by an observer comoving with the other particle). What is a bound on $|w|$?

At the point of interest, choose the orthonormal frame which gives the orbits equal and opposite 3-velocities $\boldsymbol{v}$, so that the tangent 4-velocities have components

$$\boldsymbol{u}_1 = (\gamma, -\gamma \boldsymbol{v}) , \qquad \boldsymbol{u}_2 = (\gamma, +\gamma \boldsymbol{v}) . \tag{A9}$$

The magnitude $v$ of $\boldsymbol{v}$ is related to the relative velocity $|w|$ by the velocity addition formula,

$$|w| = 2v/(1 + v^2) . \tag{A10}$$

By analogy with equation (A1) we have

$$E_1/\mu_1 = \gamma \xi_0 + \gamma \boldsymbol{v} \cdot \boldsymbol{\xi} , \qquad E_2/\mu_2 = \gamma \xi_0 - \gamma \boldsymbol{v} \cdot \boldsymbol{\xi} . \tag{A11}$$

Defining an angle $\eta$ by $\boldsymbol{v} \cdot \boldsymbol{\xi} \equiv v\xi \cos \eta$, and solving equation (A11) for ${\xi_0}^2$ and $\xi^2$, we obtain

$${\xi_0}^2 = (E_1/\mu_1 + E_2/\mu_2)^2/(4\gamma^2) , \tag{A12a}$$

$$\xi^2 = (E_1/\mu_1 - E_2/\mu_2)^2/(4\gamma^2 v^2 \cos^2 \eta) . \tag{A12b}$$

Subtraction of (A12b) from (A12a) yields

$$\begin{aligned} (E_1/\mu_1 - E_2/\mu_2)^2 &= [(E_1/\mu_1 + E_2/\mu_2)^2 + 4\gamma^2 \boldsymbol{\xi}_t \cdot \boldsymbol{\xi}_t] v^2 \cos^2 \eta \\ &\leq [(E_1/\mu_1 + E_2/\mu_2)^2 + 4\gamma^2 \boldsymbol{\xi}_t \cdot \boldsymbol{\xi}_t] v^2 . \end{aligned} \tag{A13}$$

This inequality can be solved for $v$; the result is

$$v^2 \geq \left[ \frac{E_1/\mu_1 - E_2/\mu_2}{({E_1}^2/{\mu_1}^2 + \boldsymbol{\xi}_t \cdot \boldsymbol{\xi}_t)^{1/2} + ({E_2}^2/{\mu_2}^2 + \boldsymbol{\xi}_t \cdot \boldsymbol{\xi}_t)^{1/2}} \right]^2 . \tag{A14}$$

By equation (A8), the quantities appearing inside the square roots are guaranteed to be positive.

To apply equation (A14) to the question of energy extraction in the Kerr geometry, we note that for all $\theta$, $\varphi$, and $r \geq r_+$, $|\boldsymbol{\xi}_t \cdot \boldsymbol{\xi}_t| \leq 1$. If we take $E_1/\mu_1 = 3^{-1/2}$ (the minimum energy of a plunge orbit which can result from the decay of a bound, stable orbit

around any rotating black hole) and $E_2 = 0$ (the boundary of the negative energy region), we obtain

$$v \geq 2 - 3^{1/2}; \tag{A15a}$$

or by equation (A10),

$$|w| \geq \tfrac{1}{2}. \tag{A15b}$$

Hence, this class of all physically plausible plunge orbits is always separated from the negative energy region by at least half the speed of light. To achieve energy extraction, hydrodynamical forces or superstrong radiation reactions would have to accelerate particle fragments to more than half the speed of light in the "short" characteristic time of the plunge (see eq. [3.17] and the discussion following it).

## APPENDIX B

## BOUNDARY CONDITIONS FOR EQUATION (4.11)

At $r^* \to +\infty$ the asymptotic solutions are

$$\psi = e^{-i\omega t} e^{+im\varphi} S^m{}_l(\theta) e^{\pm ik_+ r^*}, \tag{B1}$$

where $k_+ = [W(r^* = +\infty)]^{1/2} = \omega$ (positive square root). By convention we may take $\omega$ as positive (see discussion following eq. [4.8]), so the correct solution, corresponding to outgoing waves, is the upper sign.

On the horizon, $r^* \to -\infty$, the discussion is not quite so simple. The asymptotic solutions are

$$\psi = e^{-i\omega t} e^{+im\varphi} S^m{}_l(\theta) e^{\pm ik_- r^*}, \tag{B2}$$

with $k_- = [W(r^* = -\infty)]^{1/2}$ (positive square root). Again by convention $\omega > 0$. The correct boundary condition is *not* that the wave appear ingoing in the coordinate frame (i.e., *not* necessarily the lower sign in eq. [B2]). Rather, the wave must be physically ingoing in the frame of a physical observer. Since all physical observers are related by Lorentz transformations, they will all agree on the boundary condition, and we can calculate with any convenient observer. Take an observer at constant $r$ just outside the horizon. Since he is within the ergosphere, he is dragged in the positive $\varphi$ direction with some angular velocity $d\varphi/dt = \Omega_d > 0$. This observer sees the local $t$, $r$ dependence of $\psi$ (eq. [B2]) as

$$\psi \sim e^{-i(\omega - m\Omega_d)t} e^{\pm ik_- r^*}. \tag{B3}$$

Hence, for physically ingoing waves one must choose the sign $(\pm ik_-)$ opposite to the sign of $(\omega - m\Omega_d)$. On the horizon $\Omega_d \to \omega_+ = a/(2Mr_+)$ for all observers. Hence the correct sign in equation (B2) is

if $m < 0$, lower sign $(-)$;

if $m > 0$, lower sign $(-)$ if $\omega > m\omega_+$, upper sign $(+)$ if $0 < \omega < m\omega_+$.

In the last case the waves are apparently *outgoing* in the coordinate picture, and in fact they extract rotational energy from the rotating black hole, even though they are physically ingoing in the local frame of any physical observer. This kind of wave is generated by a particle in any direct, stable circular orbit for $a = M$, and also holds for small $a$ if the particle orbit is sufficiently far out.

However, even for $a \approx M$ the highly relativistic orbits at $r \sim r_{ph}$ cannot extract energy from the black hole. When $\delta = (1 - a/M) \ll 1$ and $r = M[1 + 2(\frac{2}{3}\delta)^{1/2}]$, then

$$\Omega - \omega_+ \approx \frac{1}{2M}(1 - 3^{1/2}/2)(2\delta)^{1/2} > 0\,, \tag{B4}$$

so the particle loses energy to the black hole.

For an alternative and more rigorous discussion, the reader is referred to Misner (1972*b*).

## APPENDIX C

## BOUNDS ON EIGENVALUES OF SPHEROIDAL HARMONICS

Define the following differential operator $L$ on the closed interval $[-1, 1]$:

$$L = -\frac{d}{dx}(1 - x^2)\frac{d}{dx} + g(x)\,, \tag{C1}$$

where

$$g(x) = |c^2|(1 - x^2) + \frac{m^2}{1 - x^2} > 0\,. \tag{C2}$$

Then the oblate spheroidal harmonics ${S^m}_l(c^2, x)$, where $c^2 < 0$, are eigenfunctions of $L$ which are regular at $x = \pm 1$:

$$L{S^m}_l = \alpha_{ml}{S^m}_l\,. \tag{C3}$$

Here $m$ is fixed and $l = m, m + 1, \ldots$. In the text, we use $x = \cos\theta$, $c^2 = -a^2\omega^2$, and $\lambda_{ml} = \alpha_{ml} - |c^2|$. We use $\alpha_{ml}$ in this Appendix to make $L$ a positive operator so that various theorems are directly applicable. In this Appendix, all functions $u$ on which $L$ acts will be normalized as follows:

$$\int_{-1}^{1} u^2 dx = 1\,. \tag{C4}$$

[This differs from the normalization of ${S^m}_l$ in the rest of the paper by a factor of $2\pi$, and from the normalization used by Flammer (1957): ${S^m}_l$(here) $= {N_{mn}}^{-1/2}S_{mn}$(Flammer). Flammer (1957) tabulates the conventions used by various authors.]

Let $u$ be a trial function for equation (C3). As Friedman (1956) shows, an upper bound $\rho$ for the lowest eigenvalue, $\alpha_{mm}$, is given by

$$\rho = \int_{-1}^{1} uLu dx\,, \tag{C5}$$

while a lower bound is

$$\rho - \left[\int_{-1}^{1} (Lu)^2 dx - \rho^2\right]^{1/2}. \tag{C6}$$

Taking as a trial function the associated Legendre function $u = {P^m}_l$ and using the identity

$$x{P^m}_l(x) = \frac{l - m + 1}{2l + 1}{P^m}_{l+1}(x) + \frac{l + m}{2l + 1}{P^m}_{l-1}(x) \tag{C7}$$

to perform the integrals, we find

$$l(l+1) - \frac{|c|^2}{2l+3}\left[1 + 2\left(\frac{l+1}{2l+5}\right)^{1/2}\right] \leq \lambda_{ll} \leq l(l+1) - \frac{|c|^2}{2l+3}\,. \tag{C8}$$

The right-hand side of this inequality gives the upper bound quoted in § IV,

$$\lambda_{ll} \leq l(l+1)\,. \tag{C9}$$

Since $|c|^2 = a^2m^2\Omega^2$, and $\mathscr{Y}^2 \leq 1$ implies $a^2\Omega^2 \leq \frac{1}{4}$, the left-hand side of inequality (C8) gives

$$\lambda_{mm} \geq m^2\,. \tag{C10}$$

The eigenvalues of the Sturm-Liouville operator (C1) increase monotonically with $l$, hence inequality (C10) gives

$$\lambda_{ml} \geq m^2\,. \tag{C11}$$

Inequalities (C10) and (C11) are the lower bounds used in § IV.

The upper bound (C9) holds for $l \neq m$ as well, since from the theory of Sturm-Liouville equations (e.g., Courant and Hilbert 1953), if we increase $g(x)$ to a new function $g'(x)$, then the new eigenvalues $\alpha'_{ml} = \lambda'_{ml} + |c|^2$ are all greater than the old ones. Choose

$$g'(x) = |c|^2 + \frac{m^2}{1-x^2}\,. \tag{C12}$$

Then

$$\lambda_{ml} \leq \lambda'_{ml} = l(l+1)\,. \tag{C13}$$

An alternative lower bound can be derived by choosing

$$g'(x) = \frac{m^2}{1-x^2} \leq g(x)\,. \tag{C14}$$

Then

$$\lambda_{ml} \geq \lambda'_{ml} = l(l+1) - |c|^2 \geq l(l+1) - \tfrac{1}{4}m^2\,. \tag{C15}$$

This inequality is stronger than the bound (C11) when $m^2 \leq \frac{4}{5}l(l+1)$.

## REFERENCES


Bardeen, J. M. 1970*a*, *Nature*, **226**, 64.
———. 1970*b*, *Ap. J.*, **162**, 71.
Boyer, R. H., and Lindquist, R. W. 1967, *J. Math. Phys.*, **8**, 265.
Brill, D. R., Chrzanowski, P. L., Pereira, C. M., Fackerell, E. D., and Ipser, J. R. 1972, *Phys. Rev. D.*, **5**, 1913.
Carter, B. 1968*a*, *Phys. Rev.*, **174**, 1559.
———. 1968*b*, *Comm. Math. Phys.*, **10**, 280.
Christodoulou, D. 1970, *Phys. Rev. Letters*, **25**, 1596.
Courant, R., and Hilbert, D. 1953, *Methods of Mathematical Physics* (New York: Interscience Publishers), Vol. **1**, chap. 6.
Davis, M., Ruffini, R., Press, W., and Price, R. 1971, *Phys. Rev. Letters*, **27**, 1466.
Davis, M., Ruffini, R., Tiomno, J., and Zerilli, F. 1972, *Phys. Rev. Letters*, **28**, 1352.
de Felice, F. 1968, *Nuovo Cimento*, **57B**, 351.
Flammer, C. 1957, *Spheroidal Wave Functions* (Stanford: Stanford University Press).
Friedman, B. 1956, *Principles and Techniques of Applied Mathematics* (New York: John Wiley & Sons), p. 213.
Kerr, R. P. 1963, *Phys. Rev. Letters*, **11**, 237.
Lynden-Bell, D., and Rees, M. J. 1971, *M.N.R.A.S.*, **152**, 461.
Mashoon, B. 1972, unpublished Ph.D. thesis, Princeton University.

Misner, C. W. 1972*a*, *Phys. Rev. Letters*, **28**, 994.
———. 1972*b*, paper to be published.
Misner, C. W., Breuer, R. A., Brill, D. R., Chrzanowski, P. L., Hughes, H. G., and Pereira, C. M. 1972, *Phys. Rev. Letters*, **28**, 998.
Penrose, R. 1969, *Revista de Nuovo Cimento*, **1**, 252.
Press, W. H. 1971, *Ap. J.* (*Letters*), **170**, L105.
Price, R. H. 1972*a*, *Phys. Rev. D*, **5**, 2439.
———. 1972*b*, *Phys. Rev. D*, **5**, 2419.
Schreier, E., Gursky, H., Kellogg, E., Tananbaum, H., and Giacconi, R. 1971, *Ap. J.* (*Letters*), **170**, L21.
Teukolsky, S. A. 1972, *Phys. Rev. Letters* (in press).
Wade, C. M., and Hjellming, R. M. 1972, *Nature*, **235**, 271.
Weber, J. 1971, *Nuovo Cimento B*, **4**, 202.
Wheeler, J. A. 1970, Proceedings of Vatican Conference on the Role of Nuclei in the Evolution of Galaxies, 1970 April 15.
Wilkins, D. C. 1972, *Phys. Rev. D*, **5**, 814.
Zerilli, F. J. 1970, *Phys. Rev. D*, **2**, 2141.